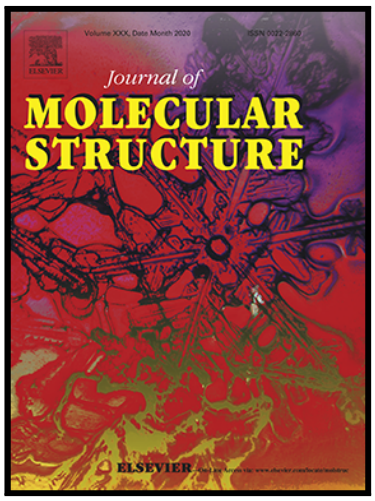

Structural and theoretical studies of 1,3-Bis-(1,2,3-triazol-1-yl)-propan-2-ol derivatives.

Armando Zambrano-Huerta , Joanatan M. Bautista-Renedo , Horacio Reyes Data Curation , Diego Martínez-Otero , Iván García-Orozco , Roberto Carlos Melgar-Fernández , María Teresa Ramírez-Palma , Nelly González-Rivas , Erick Cuevas-Yañez

PII: S0022-2860(20)31189-3
DOI: https://doi.org/10.1016/j.molstruc.2020.128864
Reference: MOLSTR 128864

To appear in: *Journal of Molecular Structure*

Received date: 22 April 2020
Revised date: 4 July 2020
Accepted date: 8 July 2020

Please cite this article as: Armando Zambrano-Huerta , Joanatan M. Bautista-Renedo , Horacio Reyes Data Curation , Diego Martínez-Otero , Iván García-Orozco , Roberto Carlos Melgar-Fernández , María Teresa Ramírez-Palma , Nelly González-Rivas , Erick Cuevas-Yañez , Structural and theoretical studies of 1,3-Bis-(1,2,3-triazol-1-yl)-propan-2-ol derivatives., *Journal of Molecular Structure* (2020), doi: https://doi.org/10.1016/j.molstruc.2020.128864

Highlights:

- The crystal structure of three 1,3-Bis-(1,2,3-triazol-1-yl)-propan-2-ol derivatives was determined by and analyzed by Single-crystal X-ray diffraction studies.

- O-H···N and C-H···N interactions in these bistriazoles are detected and promote the formation of infinite chains which define the crystal network.

- The theoretical Theoretical DFT studies show a high similarity of these compounds with Fluconazole molecule.

Structural and theoretical studies of 1,3-Bis-(1,2,3-triazol-1-yl)-propan-2-ol derivatives.

Armando Zambrano-Huerta,[1,2,3] Joanatan M. Bautista-Renedo,[1,2] Horacio Reyes,[4] Diego Martínez-Otero,[1,5] Iván García-Orozco,[2] Roberto Carlos Melgar-Fernández,[3] María Teresa Ramírez-Palma,[1,2] Nelly González-Rivas[1,2] and Erick Cuevas-Yañez[1,2]*

[1]*Centro Conjunto de Investigación en Química Sustentable UAEM-UNAM. Carretera Toluca-Atlacomulco Km 14.5, Toluca, Estado de México, 50200, México. Universidad Autónoma del Estado de México*

[2]*Facultad de Química, Universidad Autónoma del Estado de México, Carretera Toluca-Atlacomulco Km 14.5, Unidad San Cayetano, Toluca, Estado de México, C. P. 50200 México.*

[3]*Signa S.A. de C.V., Av. Industria Automotriz No. 301, Zona Industrial Toluca, Toluca, Estado de México, 50071, México*

[4]*División de Ingeniería Química, Instituto de Estudios Superiores de Jocotitlán. Carretera Toluca-Atlacomulco km 44.8, Ejido de San Juan y San Agustin, Jocotitlán, Edo. México*

[5]*Instituto de Química, Universidad Nacional Autónoma de México, Circuito Exterior S. N., Ciudad Universitaria, Coyoacán, Ciudad de México, 04510, Mexico*

*Corresponding author. Universidad Autónoma del Estado de México. Tel. +52 722 276 66 10; fax: +52 722 180 62 17, e-mail: ecuevasy@uaemex.mx.

Abstract. The crystal structure of three 1,3-Bis-(1,2,3-triazol-1-yl)-propan-2-ol derivatives was determined by X-ray diffraction analyses. The studied compounds presented O-H···N hydrogen bonds between hydroxyl group of one molecule with triazolyl nitrogen atom of another molecule. In addition, other C-H···N interactions between two bistriazole molecules are observed. These interactions promote the formation of infinite chains which define the crystal network. The results are in accordance with the solid behavior of compounds, as evidenced from XRPD and SEM studies. Theoretical studies of molecular and electronic properties using DFT (Density Functional Theory) revealed a high similarity of these compounds with Fluconazole molecule.

Keywords. 1,2,3-Triazole, Crystal structure, Density functional theory.

1. Introduction

2-(2,4-Difluorophenyl)-1,3-bis(1,2,4-triazol-1-yl)-propan-2-ol, Fluconazole (**1**), is one of the most important drugs used to treat invasive candidiasis as well as other fungal infections [1-2].

On the other hand, the analysis and determination of the precise solid form of drugs is important for pharmaceutical industry due to particular solid state structures may change physicochemical properties in drugs such as solubility, hygroscopicity and mechanical

properties which influence dosing, storage and stability [3-4]. Hence, crystal structure studies in drugs are highly desirable together to synthetic procedures development.

In this context, the wide antifungal activity of Fluconazole has prompted the development of crystalline modifications as co-crystals [5-6] and polymorphs [7-11], but also the synthesis of new Fluconazole derivatives including diverse 1,2,3-triazolyl analogues via copper-catalyzed azide-alkyne cycloaddition (CuAAC) [12-16], the most used click reaction.

In a preceding report, we informed a systematic study on the synthesis of 1,3-bis-(1,2,3-triazol-1-yl)-propan-2-ol derivatives (**2**, scheme 1) from CuAAC reaction as a novel class of Fluconazole analogues which display an outstanding selective activity against *Candida albicans* and *Candida krusei* [17]. In relation to this work, we continued our synthetic studies with emphasis in the crystal and polymorphic behavior of these compounds which is important to understand and improve biomedical applications. This paper discloses the crystal structure of three 1,3-Bis-(1,2,3-triazol-1-yl)-propan-2-ol derivatives and other properties aiming to search and develop new molecules with high antifungal activity.

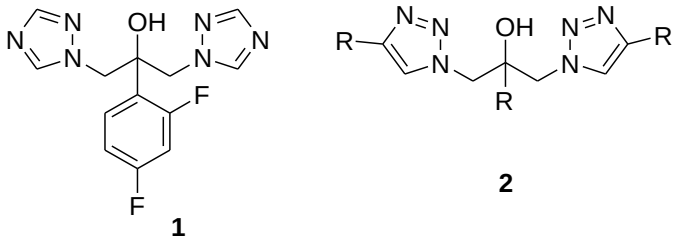

Scheme 1. Structure of Fluconazole **1** and general structure for molecules **2** proposed in this work.

2. Experimental Section

2.1. General remarks

The starting materials were purchased from Aldrich Chemical Co. and were used without further purification. Solvents were distilled before use. Silica plates of 0.20 mm thickness were used for thin layer chromatography. Melting points were determined with a Krüss Optronic melting point apparatus and they are uncorrected. ^{1}H and ^{13}C NMR spectra were recorded using a Bruker AVANCE 300; the chemical shifts (δ) are given in ppm relative to TMS as internal standard (0.00). For analytical purposes the mass spectra were recorded on a Shimadzu GCMS-QP2010 Plus in the EI mode, 70 eV, 200 °C via direct inlet probe. Only the molecular and parent ions (m/z) are reported. IR spectra were recorded on a Bruker TENSOR 27 FT instrument.

For the RX diffraction studies, crystals of compounds **5**, **6** and **8** were obtained by slow evaporation of a dilute dimethyl sulfoxifde solution, and the reflections were acquired with a Bruker APEX DUO diffractometer equipped with an Apex II CCD detector, Mo-Kα radiation (λ = 0.71073 Å) at 293 K. Three standard reflections every 97 reflections were used to monitor the crystal stability. The structure was solved by direct methods (SHELXS-97) [18] using the shelXle GUI [19]; missing atoms were found by difference-Fourier synthesis, and refined on F2 by a full-matrix least-squares procedure using anisotropic displacement parameters using SHELX-97. The hydrogen atoms of the C–H bonds were placed in idealized positions. The molecular graphics were prepared using Ortep3, POV-RAY and GIMP [20-21]. Crystallographic data for the structure reported in this paper have been deposited with the Cambridge Crystallographic Data Centre, CCDC

(No. 2013800 for compound **5**, No. 2013802 for compound **6** and No. 2013805 for compound **8**). Copies of available materials can be obtained free of charge on application to the Director, CCDC, 12 Union Road, Cambridge CB2 IEZ, UK (facsimile: (44) 01223 336033); e-mail: deposit@ccdc.ac.uk.

2.2. General procedure for the synthesis of 1,3-Bis-(4-cyclopropyl-1,2,3-triazol-1-yl)-2-arylpropan-2-ol derivatives.

1,3-dichloroacetone (2.0 g, 16.0 mmol) was added to a stirred mixture of NaN_3 (5.2 g, 7.98 mmol) and acetone (30 mL), and the resulting mixture was stirred at room temperatura for 12-15 h. The mixture was filtered, and the solvent was removed under reduced pressure. The compound was extracted with methyl tert-butyleter (2 X 30 mL), the organic layers were joined and dried over Na_2SO_4 and the solvent was removed under reduced pressure to yield 1,3-diazido-propan-2-one as a pale solid (2.1 g, 14.34 mmol, 91 %) which was used without purification. A solution of 4-fluorophenylmagnesium bromide (3.4 g, 15.91 mmol, 2.0 M in THF) and CH_2Cl_2 (15 mL) was cooled to -75°C. A solution of 1,3-diazido-propan-2-one (2.13 g, 15.91 mmol) in CH_2Cl_2 (15 mL) was added dropwise and the resulting mixture was stirred under an inert atmosphere at -75°C for 4 h and at room temperature for 24 h. A saturated solution of NH_4Cl (40 mL) was added and the mixture was stirred for 30 min. The organic layer was separated, and the aqueous phase was extracted with CH_2Cl_2 (3 X 15 mL). The organic layers were joined and dried over Na_2SO_4 and the solvent was removed under reduced pressure to yield the corresponding 1,3-diazido-2-arylpropan-2-ols **2** and **3** which were used without purification. A solution of cyclopropylacetylene (1.12 g, 17.0 mmol) in MeOH (15 mL) was added to a solution of the appropriate 1,3-diazido-2-arylpropan-2-ol (11.43 mmol) in MeOH (10 mL). The mixture

was stirred at room temperature for 5 min, a 2 N solution of NaOH (2 mL, 0.160 g, 4.0 mmol) and CuI (0.3063 g, 2.29 mmol) were successively added, and the resulting mixture was stirred at room temperature for 24 h. The solvent was removed under reduced pressure and concentrated NH_4OH solution (40 mL) was added and the mixture was stirred for 2 h. The product was filtered, washed with H_2O (20 mL) and cold MeOH (20 mL), and dried under reduced pressure to afford the corresponding1,3-bis-(4-cyclopropyl-1,2,3-triazol-1-yl)-2-arylpropan-2-ol derivative which was purified by crystallization.

2.2.1. 1,3-Bis-(4-cyclopropyl-1,2,3-triazol-1-yl)-2-(4-fluorophenyl)-propan-2-ol (5). Cyclopropylacetylene and 1,3-diazido-2-(4-fluorophenyl)propan-2-ol afforded 1,3-Bis-(4-cyclopropyl-1,2,3-triazol-1-yl)-2-(4-fluorophenyl)-propan-2-ol (**5**) as white solid (90 %), m.p. 235 °C. ^{1}H NMR (300 MHz, DMSO-d_6) δ 8.31 (s, 2H), 7.4 (d, *J* = 7.3 Hz, 2H), 7.1 (d, *J* = 7.5 Hz, 2H), 6.47 (s, broad, 1H), 4.98 (d, *J* = 14.1 Hz, 2H), 4.81 (d, *J* = 14.3 Hz, 2H),), 2.03 (m, 2H), 1.01 (d, 2H), 0.08 (d, 2H); ^{13}C NMR (75 MHz, DMSO-d_6) δ 163.5 (d, 1 X C, $J_{C\text{-}F}$ = 241 Hz), 146.2 (2 X C), 136.9 (1 X C), 128.3 (2 X CH), 125.6 (2 X CH), 115.3 (2 X CH), 75.1 (1 X C), 57.6 (2 X CH_2), 8.2 (4 X CH_2), 7.0 (2 X CH); IR (ATR, cm^{-1}): 3164, 3147, 2970, 2948, 1603; MS [EI+] m/z (%): 368 $[M]^+$ (5). HRMS (EI): calcd. For $C_{19}H_{21}FN_6O$: 368.1761; found: 368.1771.

2.2.2. 1,3-Bis-(4-cyclopropyl-1,2,3-triazol-1-yl)-2-(4-chlorophenyl)-propan-2-ol (6). Cyclopropylacetylene and 1,3-diazido-2-(4-chlorophenyl)-propan-2-ol afforded 1,3-Bis-(4-cyclopropyl-1,2,3-triazol-1-yl)-2-(4-chlorophenyl)-propan-2-ol (**6**) as white solid (80 %), m.p. 240 °C. ^{1}H NMR (300 MHz, DMSO-d_6) δ 7. 68 (s, 2H), 7.66 (d, 4H), 7.52 (d, 4H), 6.41 (s, broad, 1H), 4.89 (d, *J* = 14.2 2H), 4.63 (d, *J* = 14.1 Hz, 2H), 2.03 (m, 2H), 1.01 (d,

2H), 0.08 (d, 2H); ^{13}C NMR (75 MHz, DMSO-d_6) δ 148.8 (2 X C), 139.9 (1 X C), 137.3 (1 X C), 132.7 (2 X CH), 128.4 (2 X CH), 122.6 (2 X CH), 75.3 (1 X C), 57.6 (2 X CH_2), 8.2 (4 X CH_2), 7.0 (2 X CH); IR (ATR, cm^{-1}): 3149, 3090, 2970, 2948, 1597; MS [EI+] m/z (%): 384 $[M]^+$ (5). HRMS (EI): calcd. For $C_{19}H_{21}ClN_6O$: 384.1465; found: 384.1468.

2.3. 1,3-bis(4-phenyl-1,2,3-triazol-1-yl)propan-2-ol (8). According to literature [22], a solution of 1,3-diazidopropan-2-ol (0.284 g, 2 mmol) in MeOH (3.0 mL), prepared form epichlorohydrin **7** [23] was added to a stirred mixture of phenylacetylene (0.214 g, 2.1 mmol), a 0.5 N solution of NaOH (0.5 mL, 0.25 mmol) and CuI (0.019 g, 0.1 mmol) in MeOH (2.0 mL). The reaction mixture was stirred at room temperature for 24h. The reaction mixture was filtered through celite, and the solvent was removed *in vacuo*. The final product was purified by column chromatography (SiO_2, hexane/AcOEt 8:2) to afford compound **8** as a white solid (91%); mp 196-197°C. ^{1}H NMR ($CDCl_3$, 300 MHz) δ 8.53 (s, 2H), 7.85 (d, *J* = 7.5 Hz, 4H), 7.43 (t, *J* = 8 Hz, 4H), 7.31 (t, *J* = 7.5 Hz, 2H), 5.78 (d, *J* = 5 Hz, 1H), 4.60 (d, *J* = 10.5 Hz, 2H), 4.41 (d, *J* = 10.5 Hz, 2H); ^{13}C NMR ($CDCl_3$, 75 MHz) δ 146.1, 130.8, 128.8, 127.7, 125.0, 122.4, 68.2, 53.2; IR (ATR, cm^{-1}): 3220, 3080, 1455, 1600; MS (EI+) m/z (%) 346 [M]+ (100).

2.4. Computational details

With the aim to study the influence of substitutions made on compounds 5 and 6 presented in Scheme 2, theoretical estimations on the framework of Density Functional Theory, DFT, were performed at the PBE0/3-21G level of theory implemented in the computational software NWChem 6.5 [24]. These compounds were compared with hypothetical substitutions as exemplified in Scheme 2. Global descriptors like ionization potential [25],

IP, electron-affinity [26], **EA**, and softness [27], ***S***, as well as some local descriptors like dual descriptor [28] denoted as f^2, and Molecular Electrostatic Potential [29], **MEP**, were used to characterize the internal reactivity. The obtained results were compared with those presented for fluconazole structure [30]. For purposes of theoretical analysis, all substituents in the structures were labeled as S1 and S2. For example, the designation of compounds 5 and 6 would be 2.D and 2.C.

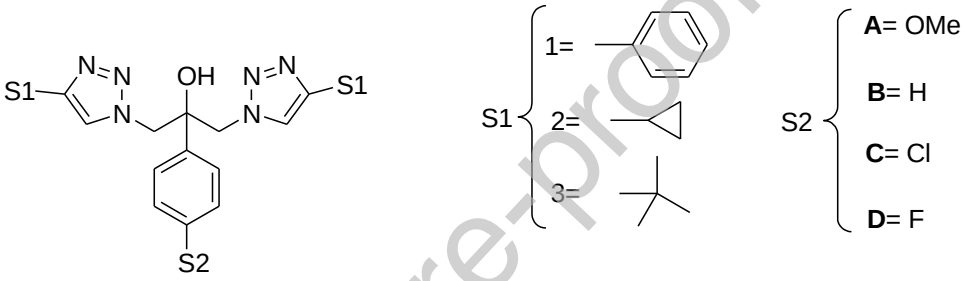

Scheme 2. Proposed structures for theoretical analysis

3. Results and discussion

3.1 Chemistry

Bistriazoles **5** and **6** are representative examples of 1,3-bis-(1,2,3-triazol-1-yl)-propan-2-ol derivatives bearing a cyclopropyl group with a remarkable antifungal activity against *Candida albicans* and *Candida krusei* strains (MIC= 0.0075 μg/mL for compound **5**, and MIC= 0.04 μg/mL for compound **6**). These compounds were obtained from the CuAAC reaction of cyclopropylacetylene **4** with the corresponding 1,3-diazidopropan-2-ol derivatives **2** and **3** in presence of catalytic amounts of CuI (scheme 3) [17]. Alcohols **2** and

3 were prepared from 1,3-dichloroacetone **1** which was successively treated with sodium azide and the corresponding Grignard reagent.

The global yields of these processes were close to 80 %. On the other hand, bistriazole **8** was synthesized according to the literature from epichlorohydrin [22,23].

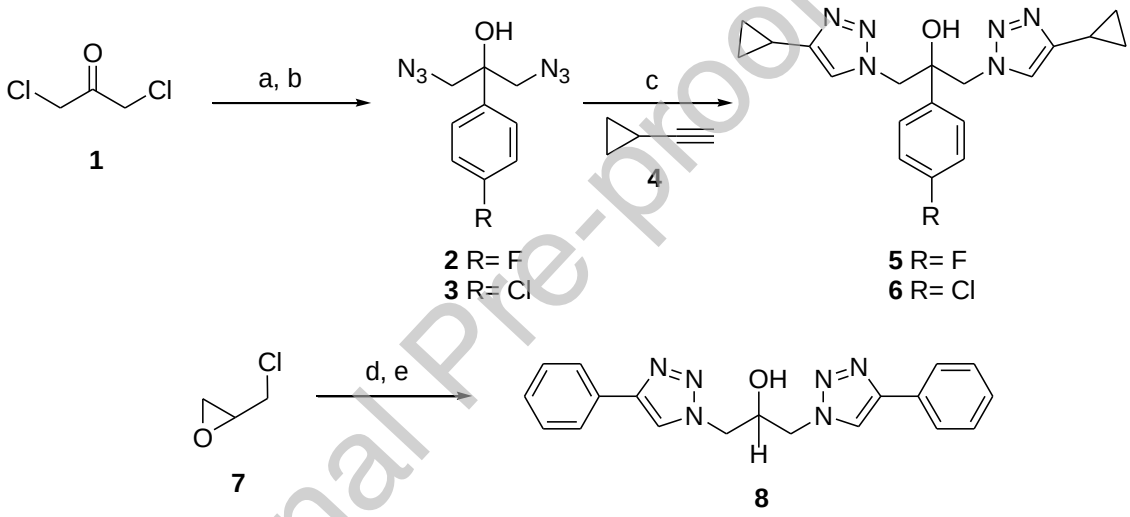

Scheme 3. Reagents and conditions: (a) NaN_3, acetone. (b) RC_6H_4MgBr, THF-CH_2Cl_2, -75°C. (c) CuI, NaOH, MeOH. (d) NaN_3, NH_4Cl, MeOH-H_2O. (e) CuI, phenylacetylene, NaOH, MeOH, RT.

3.2 Crystal Structure Analysis

Suitable crystals of compounds **5**, **6** and **8** were obtained from a DMSO solution upon slow evaporation over several days. Single-crystal X-ray diffraction studies were performed on these compounds confirming the spectroscopic results. Crystallographic data and structural refinement parameters of **5**, **6** and **8** are summarized in table 1 and selected bond lengths and angles are shown in table 2.

Table 1. Crystallographic data for structural analysis of compounds **5**, **6** and **8**.

Crystal data	**5**	**6**	**8**
Empirical formula	$C_{19}H_{21}FN_6O$	$C_{19}H_{21}ClN_6O$	$C_{19}H_{18}N_6O$
Formula weight	368.42	384.87	346.39
Temperature(K)	293(2) K	296(2) K	100(2)
Radiation type	Mo *Kα*	Mo *Kα*	Mo *Kα*
Crystal system	Monoclinic	Orthorhombic	Orthorhombic
Space group	$P2_1/c$	*Pbca*	*Pccn*
Unit cell dimensions (Å, °)			
a	14.5172(8)	9.7040(7)	18.06187(17)
b	9.5469(5)	14.6585(10)	5.62359(6)
c	14.3270(8)	27.158(2)	16.15266(15)
α	90	90	
β	109.261(2)	90	
γ	90	90	
Volume ($Å^3$)	1874.50(18)	3863.1(5)	1640.67(3)
Z	4	8	4
Density (calculated, Mg/m^3)	1.305	1.323	1.402
Absorption coefficient μ (mm^{-1})	0.760	1.927	0.746
F(000)	776	1616	728
Crystal size (mm^3)	0.519 x 0.229 x 0.201	0.291 x 0.156 x 0.125	0.229 x 0.129 x 0.040
Θ range (deg)	3.225 to 70.321	3.255 to 70.543	4.897 to 69.819
Index ranges	-17<=h<=16, 0<=k<=11, 0<=l<=17	-7<=h<=11, -17<=k<=17, -32<=l<=30	-21<=h<=21, -6<=k<=6, -19<=l<=19
Reflections collected	3454	23880	12848
Independent reflections	3454 [*R(int)* = ?]	3662 [*R(int)* = 0.0435]	1552 [*R(int)* = 0.0145]
Data/restraints/parameters	3454 / 117 /276	3662 / 866 /403	1552 / 1 / 126
Goodness-of-fit on F^2	1.112	1.035	1.060
Final R indices [I>2sigma(I)]	R1 = 0.0570, wR2 = 0.1825	R1 = 0.0536, wR2 = 0.1634	R1 = 0.0325, wR2 = 0.0805
R indices (all data)	R1 = 0.0628, wR2 = 0.1928	R1 = 0.0588, wR2 = 0.1699	R1 = 0.0334, wR2 = 0.0811
Largest diff. peak and hole ($e\ Å^{-3}$)	0.274, −0.301	0.369, -0.324	0.182, -0.183

Table 2. Selected bond lengths and angles of compounds **5**, **6** and **8**.

Bond	Compound **5**	Compound **6**	Compound **8**
O(1)-H(1)	0.847(17)	0.835(10)	0.839 (8)
C(1)-O(1)	1.417(2)	1.412(2)	1.344(2)
C(1)-C(2)	1.520(3)	1.532(2)	1.525(15)
C(1)-C(8)	1.538(3)	1.536(2)	1.525(15)
C(1)-C(14)	1.548(2)	1.548(3)	
C(8)-N(1)	1.454(3)	1.451(3)	1.457(8)
C(14)-N(4)	1.457(3)	1.454(3)	1.457(9)
N(1)-N(2)	1.329(2)	1.335(2)	1.348(14)
N(2)-N(3)	1.324(3)	1.307(3)	1.317(14)
N(4)-N(5)	1.339(2)	1.354(3)	1.348(14)
N(5)-N(6)	1.316(3)	1.328(6)	1.317(14)

Bistriazole **5** crystallized in monoclinic centrosymmetric $P2_1/c$ space group, with four molecules in the asymmetric unit. Two of these molecules are mirror images of each other mainly due to the relative orientation of R1, R2, and R3 rings (**5A** and **5B**, Figure 1). Taking the C-O bond as the reference of the C1 tetrahedron and the phenyl ring (R1) toward the front, the CH2-triazole moiety acts as a propeller. In the case of 1A, R1 ring is quasi-parallel to R3 (dihedral angles R1-R3 = 52.47°), and the R1, R2, and R3 "blades" twist the propeller clockwise (Λ isomer). On the other case, 1B the R1, R2, and R3

"blades" turn counter-clockwise (Δ isomer). These Δ and Λ enantiomers are present in the crystal reported structures of the fluconazole [7, 31].

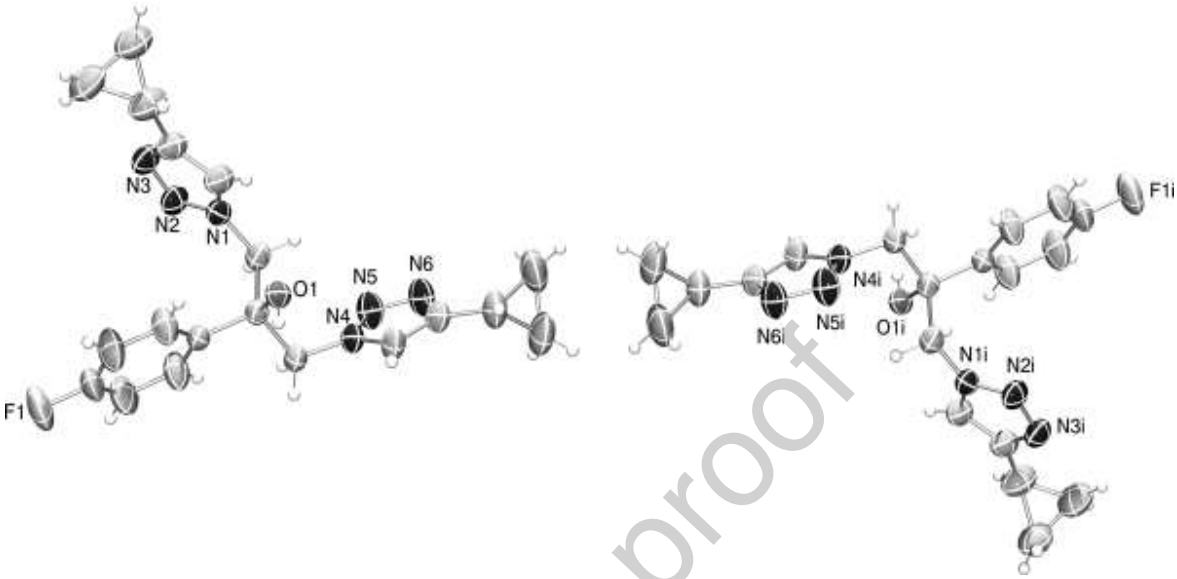

Figure 1. Enantiomers of the crystal structure of compound **5**: **5A** left, **5B** right.

Enantiomers **5A** and **5B** have an interaction through hydrogen bonding, suggesting a possible molecular recognition. Three hydrogen bond are observed by the hydroxyl and H(14) methylene groups of an A-molecule, and the R3-triazolyl ring of a B-molecule. The O-H···N hydrogen bond between the hydroxyl group of one A-molecule as donor and the R3-triazolyl N(3) nitrogen atom of one B-molecule as acceptor, is the interaction commonly observed in different fluconazole polymorphs [6, 7, 10]. Additionally, a C-H···N hydrogen bond between one of the methylene H(14) hydrogen atom of one A-molecule and the R3-triazolyl N(2) nitrogen atom. These interactions form infinite arrays parallel to the c-axis (Figure 2).

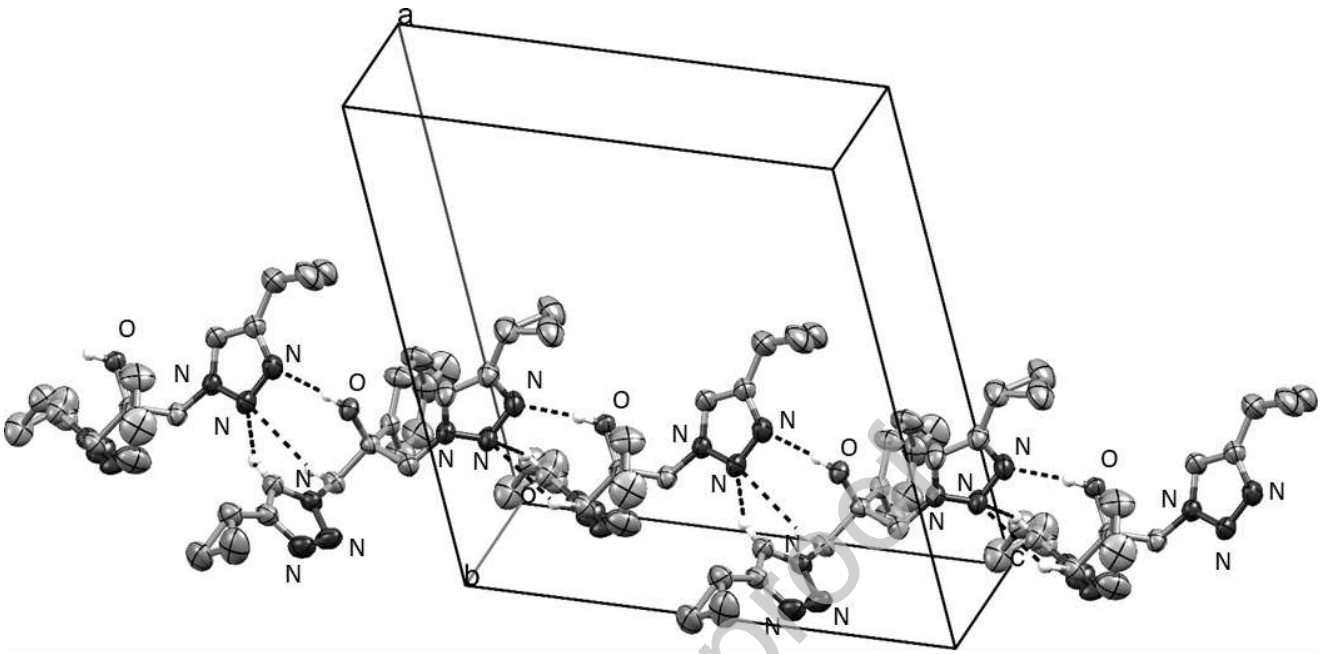

Figure 2. Infinite chain formation along b-axis by O-H···N, C-H···N and H···H interactions in B-molecules of compound **5**.

On the other hand, each A-molecule is connected by three C-H···N interactions to its similar enantiomer molecule. The R2-triazolyl ring by N(5) and N(6) nitrogen atoms interacts as a donor moiety with a methylene H(14) and phenyl H(7) hydrogen atoms of other molecule, forming an infinite array parallel to the a-axis, maintaining 21 screw axis symmetry (Figure 3). The same arrays are forming by the B-molecules.

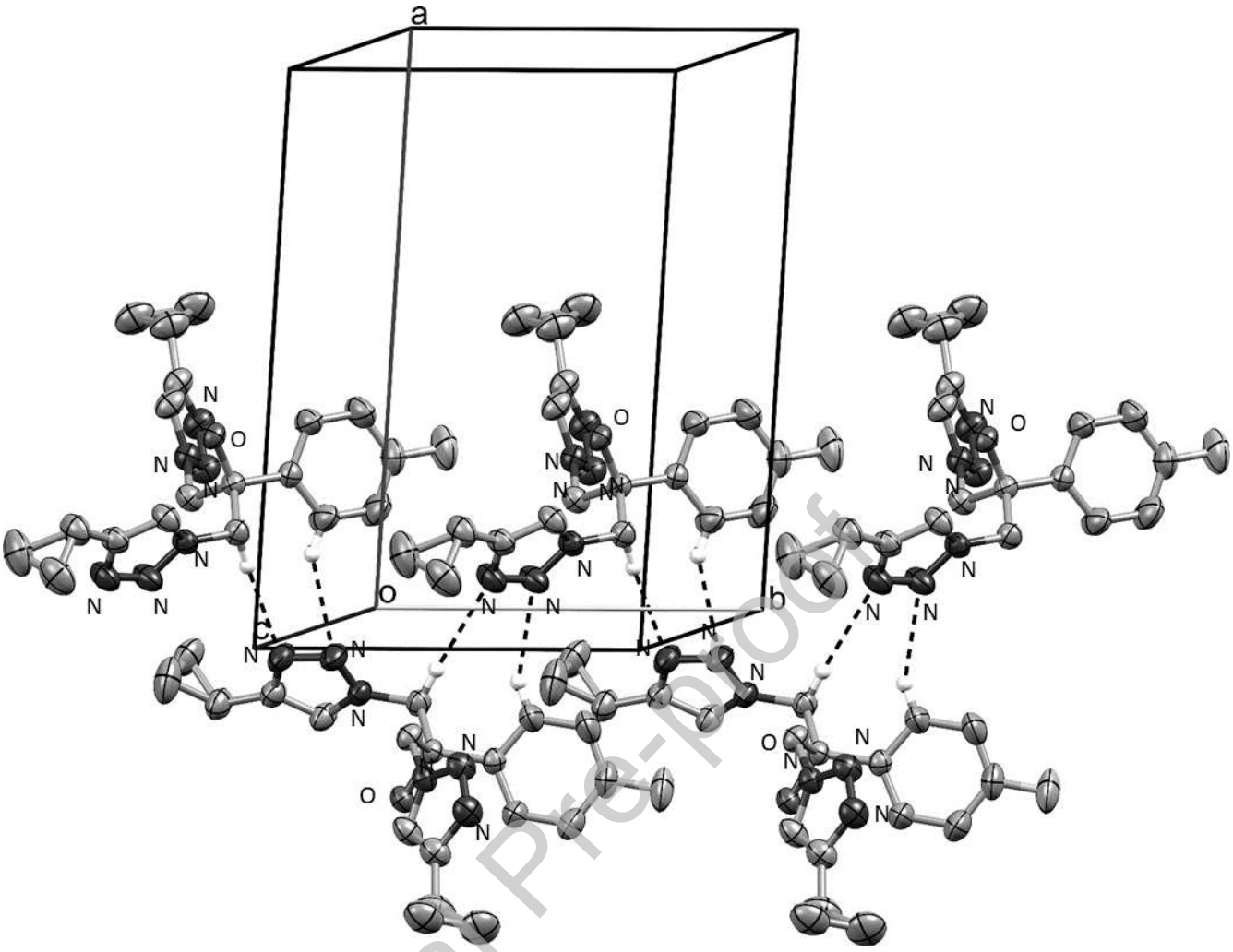

Figure 3. Infinite chain formation along b-axis by C-H···N interactions, in B-molecules of compound **5**.

The experimental powder X-ray diffraction pattern is in close agreement with the computed from single crystal X-ray analysis (Figure 4), indicating that powder presents the same phase observed in the single crystal, and only one polymorph exclusively is yielded. A noteworthy feature on the powder pattern is the increase of the relative intensities of the peaks at 12.92, 15.90 and 21.56 2-theta values respecting the single crystal peaks, which were assigned to hkl reflections (200), (210) and (310), respectively. On the other hand, the peaks at 20.80, 21.78 and 26.92 2-theta values, corresponding to hkl reflections (113),

(013) and (403) respectively decrease their intensity in respect with single crystal pattern (Figure 4). This suggests a slightly deformation in the crystalline arrangements of the powder with respect to the single crystal.

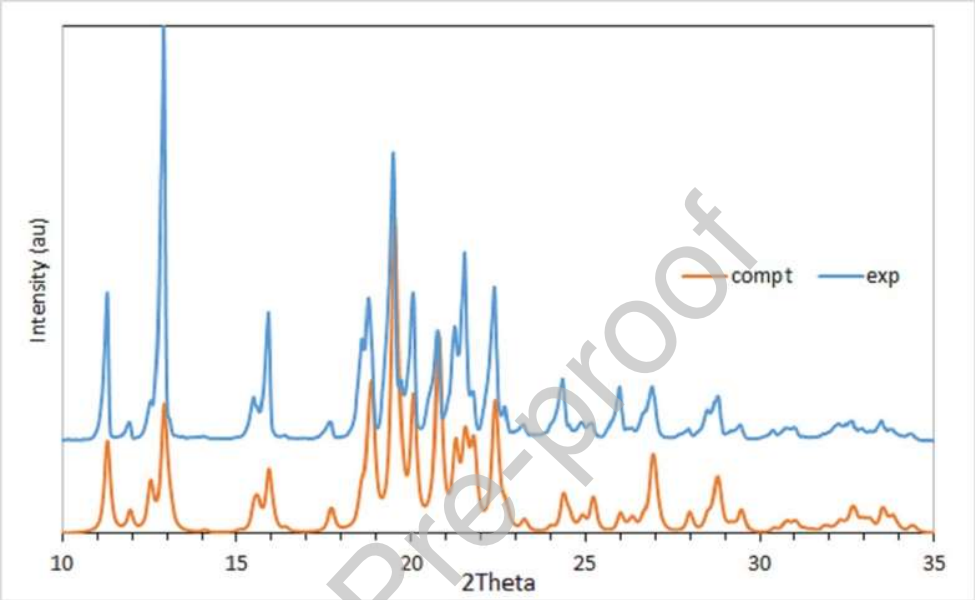

Figure 4. Diffraction patterns of compound **5**, blue line: experimental PXRD pattern, orange line: computed pattern from the single crystal data.

Compound **6** crystallizes in monoclinic centrosymmetric *Pbca* space group, with eight molecules in the asymmetric unit. The crystal cell shows the presence of mirror images of the molecule (Λ and Δ enantiomers). Molecule **6** is similar to **5**. The conformation and bond lengths of both molecules are similar, as shown with the molecular overlay (Figure 5) and the comparison of torsion angles (Table 2).

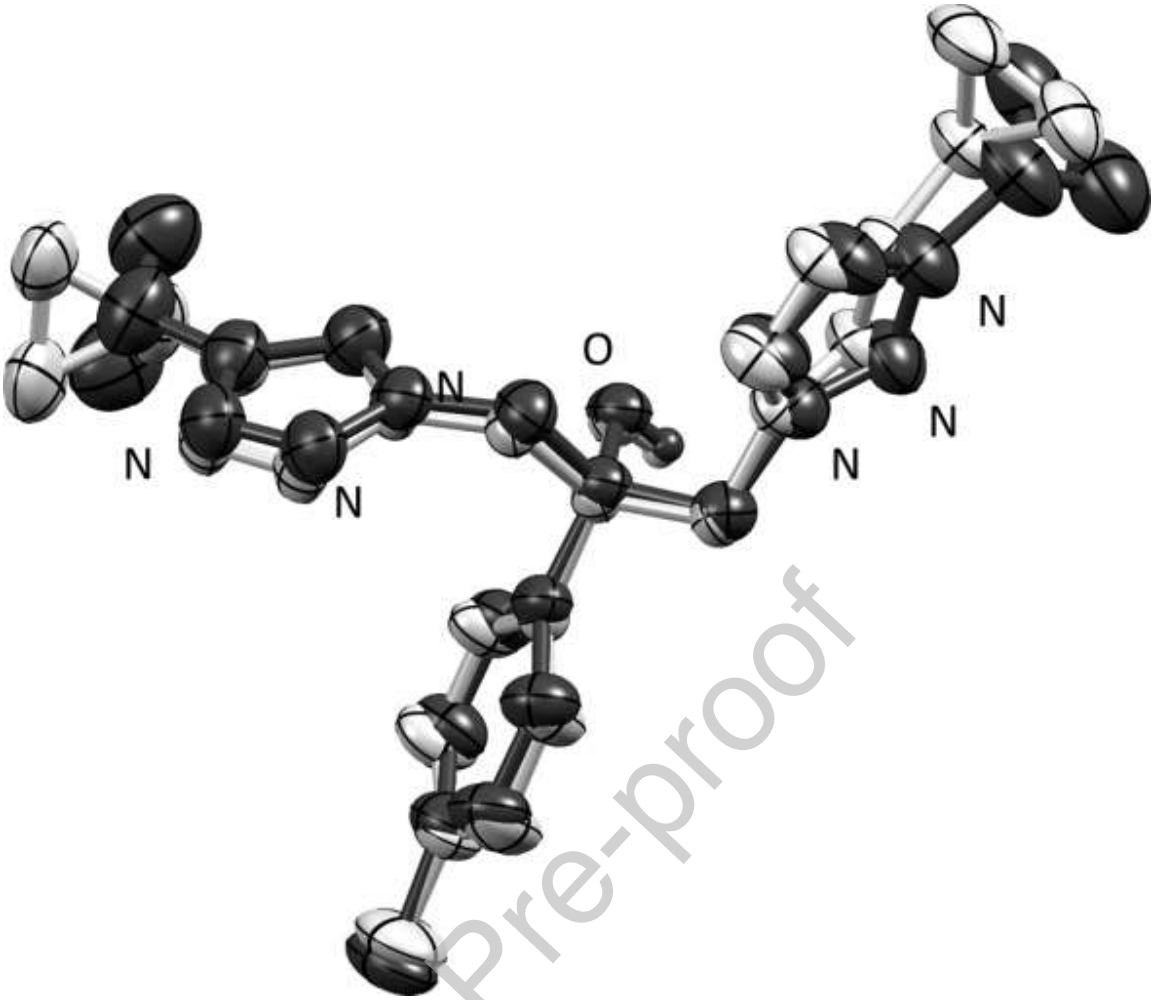

Figure 5. Molecular overlay of molecule **5** (light green) and **6** (black).

As shown for compound **5**, each Λ enantiomer of compound **6** interacts by hydrogen bonding with the Δ enantiomer (Figure 6). The R3-triazolyl ring forms two hydrogen bonds with the hydroxyl group and C14-methylene, as well as an H···H interaction between the phenyl ring and cyclopropane ring in an infinite array parallel to the b-axis. This interaction could be important due to cyclopropyl moiety is involved in modulation of drug properties, such as including potency, receptor subtype selectivity, bioavailability, half-life, microsomal stability, brain permeability, adaptation to entropically favorable binding, lipophilicity decreasing, among others, as a result of the small strained cyclopropane ring

structure which increases the applications of a drug molecule to be therapeutically useful in medicinal chemistry [32-36].

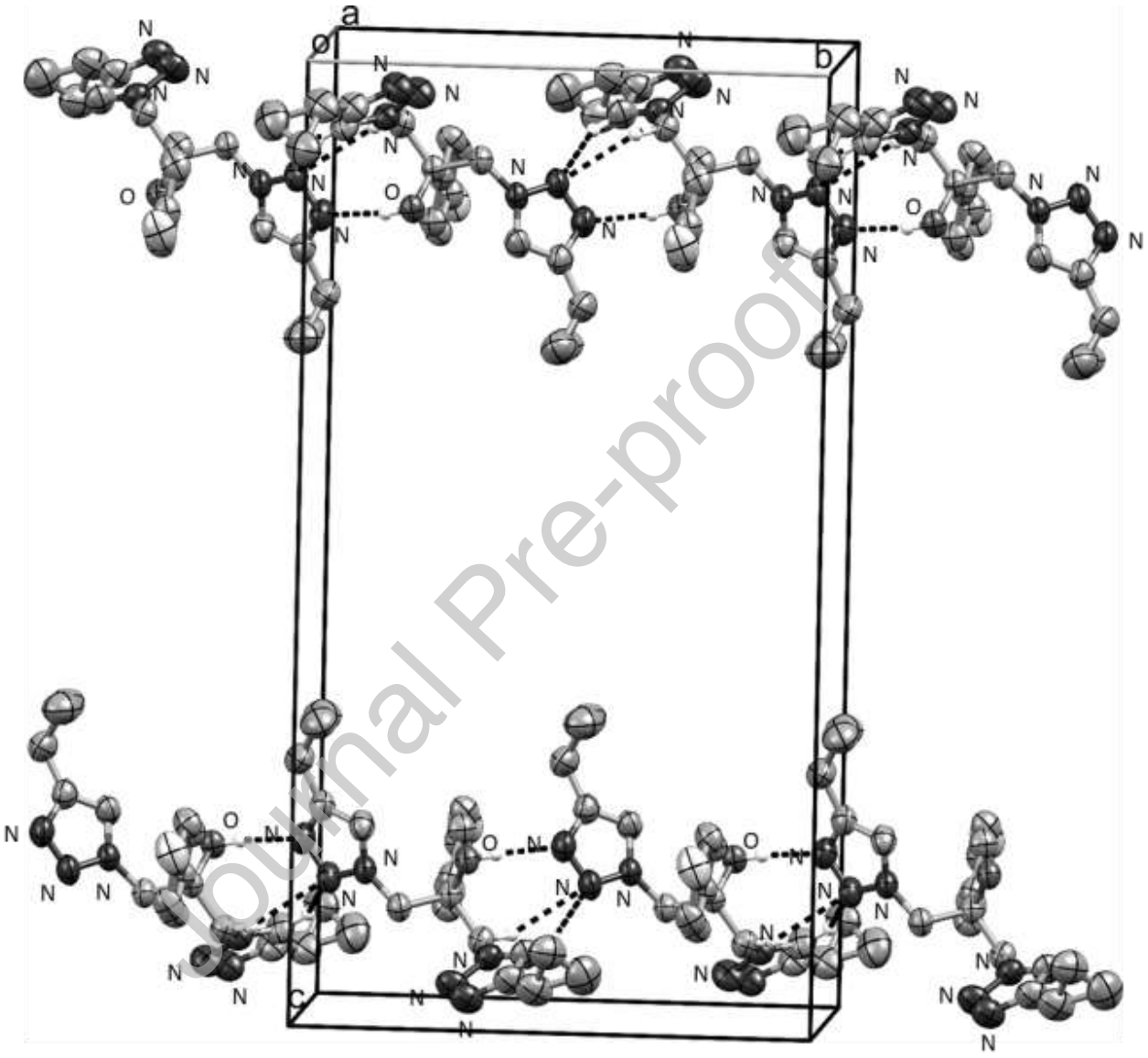

Figure 6. Infinite chain formation along b-axis by O-H···N, C-H···N and H···H interactions in B-molecules of compound **6**.

Each A or B molecule has three CH···N interactions with the same enantiomer, similar to molecule **5** (Figure 7). In addition, 21 screw symmetry is observed along the a-axis, forming an infinite array of 2A or 2B molecules. However, the hydrogen bonding for compound **6** is shorter than those observed for compound **5**, in spite of the volume of fluorine atom versus chloride atom (Table 3). Consequently, hydrogen bonding interactions are stronger in compound **6** than in compound **5**.

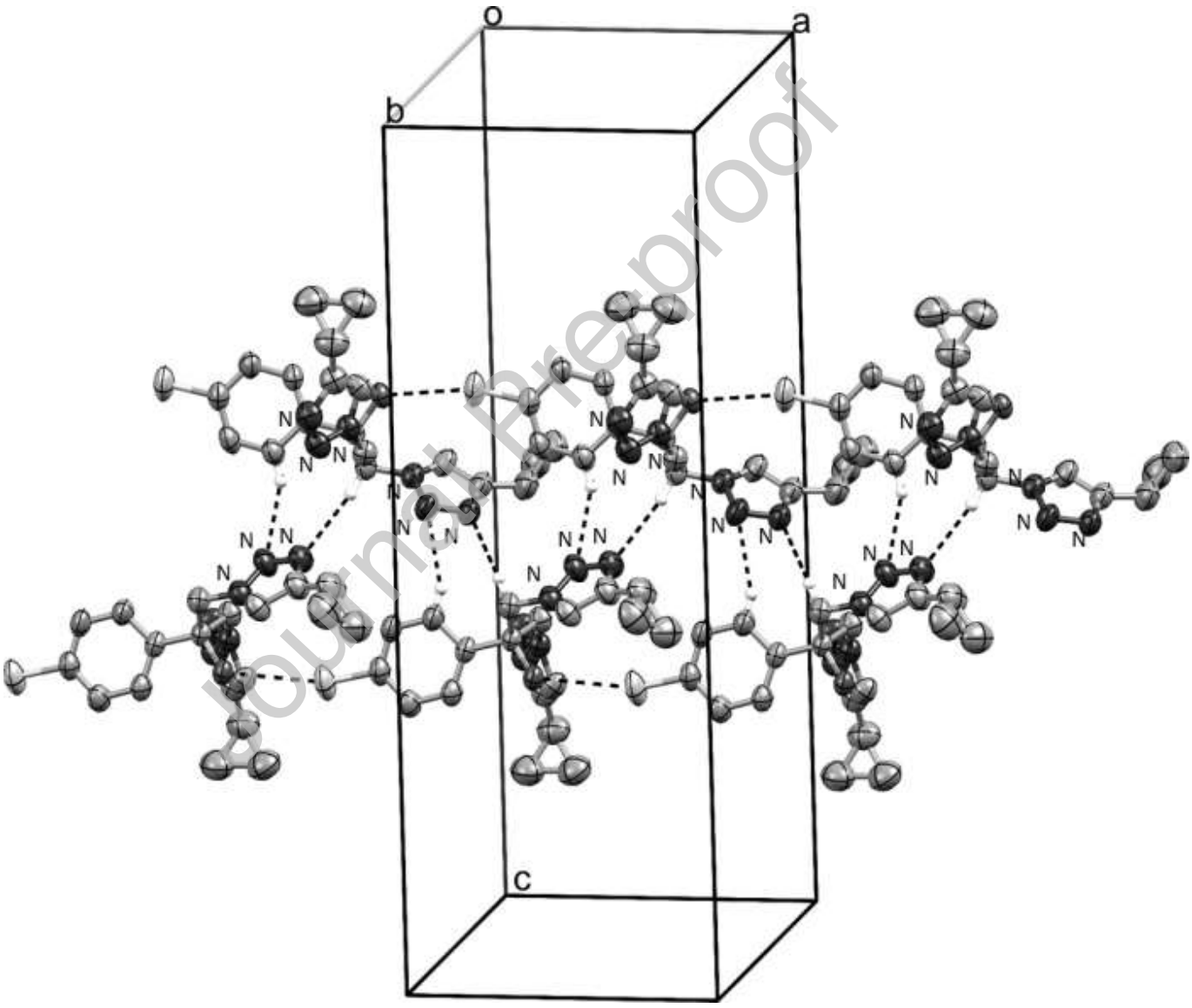

Figure 7. Infinite chain formation along a-axis by C-H···N interactions, in B-molecules of compound **6**.

An important fact in compound **6** crystal structure is the presence of a chlorine-oxygen interaction (Figure 7). The Cl···O distance is 4.812 Å which is shorter than the sum of van der Waals radii (3.20 Å). In the case of compound **5**, the distance F···O (5.036 Å) is larger than the sum of van der Waals radii (3.00 Å). Thus, the main interaction in the crystal is the hydrogen bonding as shown above, although the substituent in phenyl ring plays an important role on the crystal structure. This suggests a possible anion recognition of the triazolyl rings toward a chloride such as other groups have observed [37-39]. In this regard, an anion/π-like interaction was evaluated considering the parameters presented in table 3. The distance of chlorine atom to the computed centroid of R2-triazolyl ring is shorter than fluorine atom-triazolyl ring distance. Furthermore, the slide-angle β has the minor value in compound **6**, evidencing a strong interaction of chlorine atom with triazolyl ring.

Table 3. Parameters of the anion/π-like interaction of compounds **5** and **6**.

R2…X	Ω…X (Å)	Ω…C (Å)	α (°)	β (°)
X = F (**1**)	4.111	4.483	65.5	9.47
X = Cl (**2**)	3.926	4.516	59.39	4.48

The calculated and experimental X-ray diffraction patterns of compound **6** were compared in order to identify a possible polymorphism. The powder patterns have the same phase and the relative intensities of the peaks, indicating the presence of only one polymorph similar to the case of compound **5** (Figure 8).

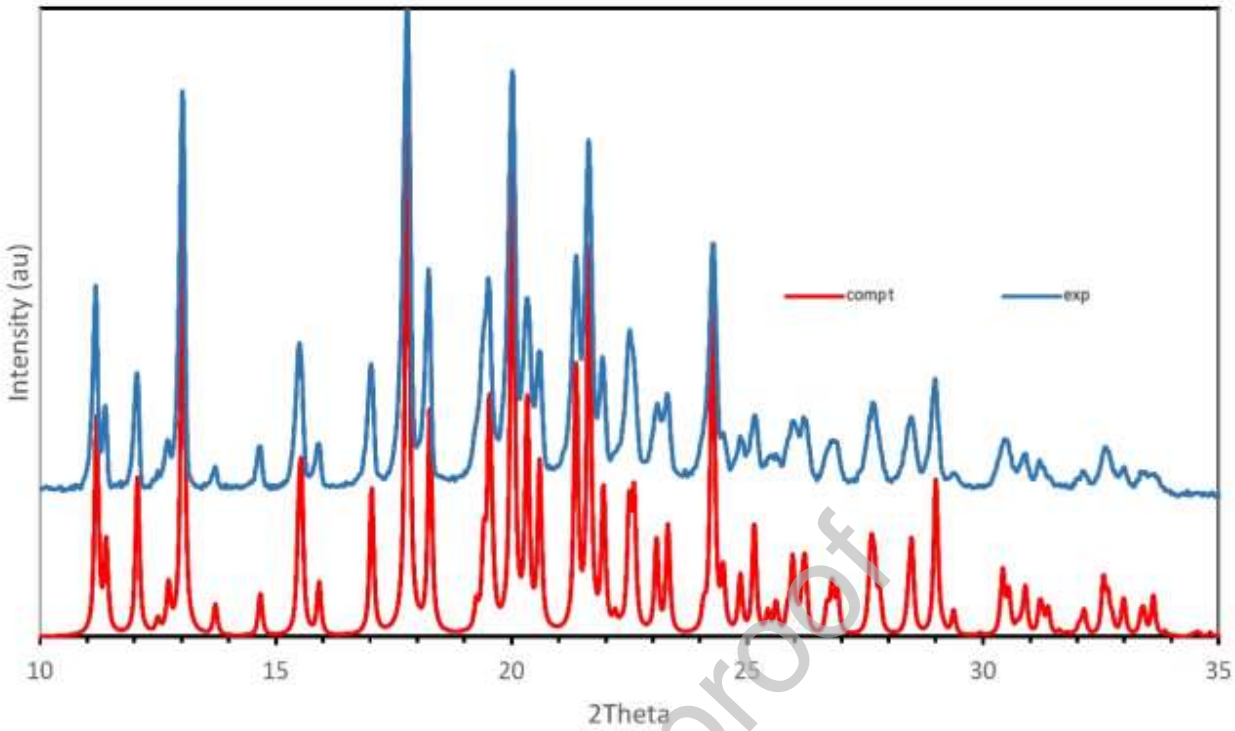

Figure 8. Diffraction patterns of compound **6**, blue line: experimental X-ray powder diffraction, red line: computed diffraction pattern.

Compounds **5** and **6** were analyzed by SEM to investigate morphologic features. While SEM micrograph obtained from compound **6** does not present some specific supramolecular aggregation with irregular shape and size and piled up disorderly (figure 9b), micrograph of compound **5** would suggest the formation of aggregates with a rectangular-shaped morphology (Figure 9a). The configuration of supramolecular aggregates with well-defined architectures using 1,3-bis-(1,2,3-triazol-1-yl)-propan-2-ol in the synthesis of copper complexes has been described and suggests that these compounds might be candidates as building blocks to integrate specific supramolecular structures [40].

(a) 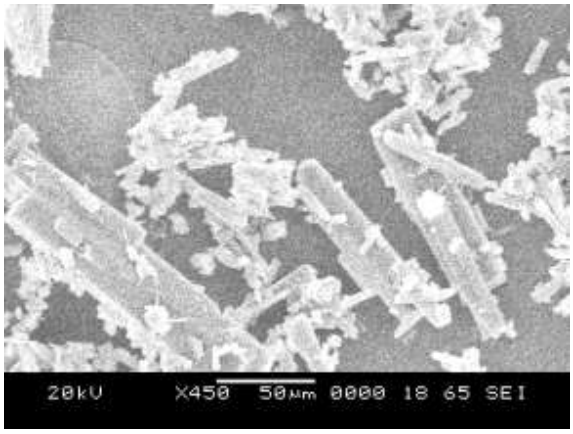

(b) 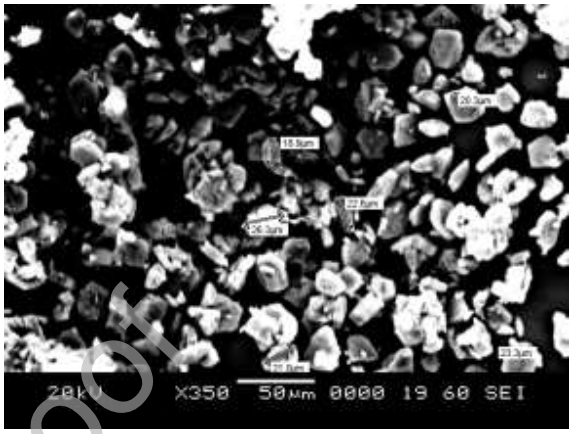

Figure 9. SEM micrographs compound **5**, (a) X450, 50 µm, and compound **6**, (b) X600, 20µm.

On the other hand, compound **8** crystallized in orthorhombic crystalline system in the *Pccn* space group. Only a half of molecule is refined, the other half is generated by the symmetry operation 1/2-x, 3/2-y, +z as observed in Figure 10. The carbon C1 is localized in a 2-fold rotation axis and a glide plane. The atoms in the alcohol moiety, oxygen O1 and hydrogen H1a, as well as hydrogen atom bonded to carbon C1 were treated as a disorder in special position using the PART -1 instruction and the occupancy was fixed in 0.5.

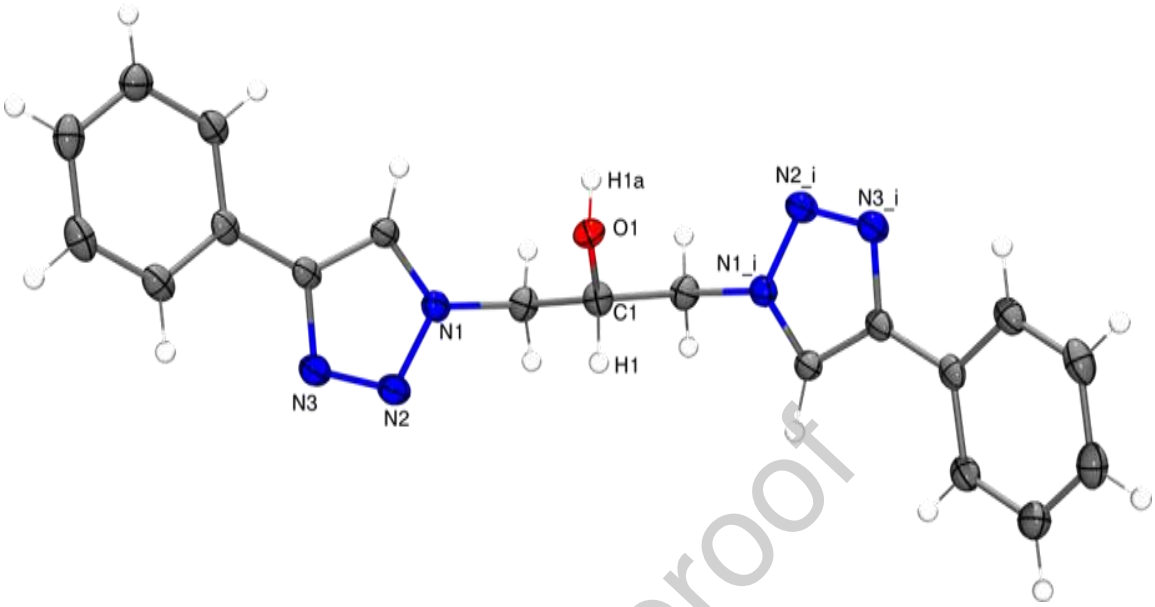

Figure 10. ORTEP diagram for compound **8**, Symmetry transformations used to generate equivalent atoms: 1/2-x, 3/2-y, +z, the atoms O1, H1a and H1 generated by symmetry are omitted by clarity.

The O-H group forms hydrogen bonds type (a) with a distance of 2.006(12) Å between hydrogen H1a and nitrogen N(2) (Table 4), along the a-axis forming a unidimensional net through an infinite array similar to compounds **5** and **6**. In general, these hydrogen bonds can be described as C2,2(12) >a<a forming a 12-membered chain (Figure 11a). A 12-membered ring is also observed in the packing between two adjacent molecules described in terms of graph set as R2,2(12) >a>a (Figure 11b).

Table 4. Hydrogen bonds for **8** [Å and °].

D-H...A	d(D-H)	d(H...A)	d(D...A)	<(DHA)
O(1)-H(1A)...N(2)#1	0.84(1)	2.006(12)	2.8268(18)	165(3)

Symmetry transformations used to generate equivalent atoms: #1 x,y-1,z

(a)

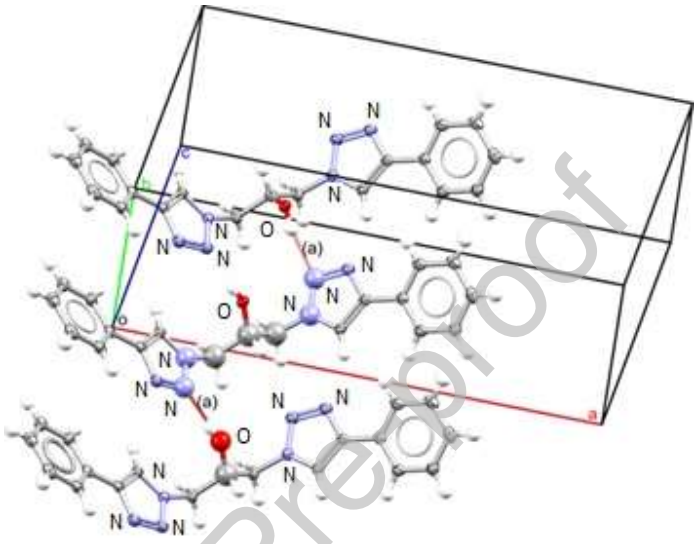

(b)

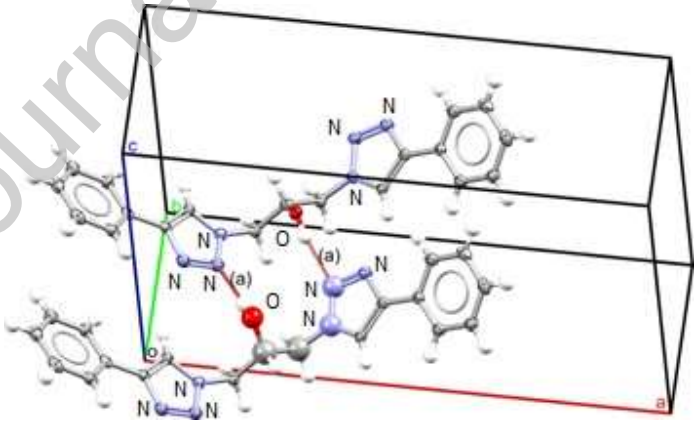

Figure 11. Hydrogen bonds observed in packing of compound **8**: a (up) 12-membered chain, b (down) 12-membered ring.

3.3 Computational analysis

3.3.1. Effects of S1 substituent in the molecular reactivity

In figure 12 are presented some representative optimized structures [24], these structures shown the formation of an internal hydrogen-bond between the benzyl alcohol and one of the heterocyclic rings. This conformation inflicts modifications in the internal reactivity of the molecule. In figure 13, we present the Molecular Electrostatic Potential, MEP, projected on the electron density for one of the proposed compounds.

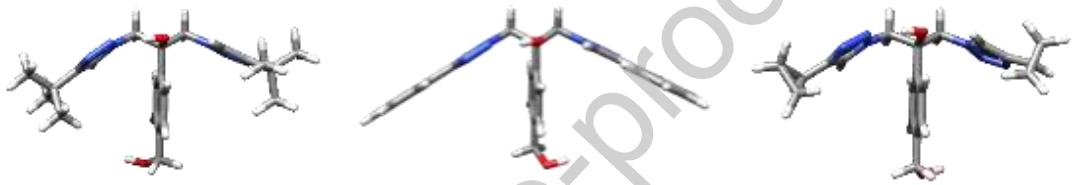

Figure 12. Optimized structures for some selected bis-1,2,3-triazoles obteined with the PBE0/3-21G method.

Molecular Electrostatic Potential, MEP, surfaces illustrate the charge distributions of a given molecule in a three-dimensional space, allowing to visualize positive, neutral and negative charge regions. In figure 13, the MEP projected upon an iso-surface of electron density of compounds 2.D and Fluconazole is presented as example of the behavior of all compounds studied. Positive, neutral and negative charge regions are indicated in red, green and blue respectively. The charge distribution presented in MEP shows a positive region located upon the aromatic hydrogen of one of heterocycles while in the same ring an irregular negative charge distribution is observed upon aromatic nitrogen atoms of which one of them participates in the hydrogen bond. In contrast with the behavior of opposite

heterocyclic ring that shown a uniform negative charge distribution of aromatic nitrogens. Similar results are observed in the MEP of fluconazole structure, so the set of compounds presented is expected to show similar pharmacological activity to fluconazole. Regarding to the effect of the S1 substituent, no appreciable influence is observed.

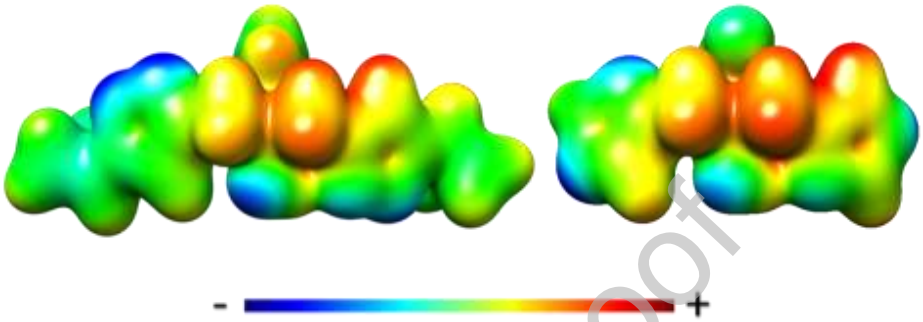

Figure 13. Representative molecular electrostatic potential, MEP, mapped on the electron density surface with iso value of 0.01 a.u., for the set of proposed structures and for fluconazole structure calculated with the PBE0/3-21G method. The color scales from blue to red illustrating the charge distribution with values of -0.005 a.u. to 0.005 a.u. respectively.

The formation of the intra-molecular hydrogen bond not only is reflected on the MEP behavior. In figure 14, we present the Dual descriptor projected on the electron density, where red and blue regions refer to positive and negative values of f^2. The chemical meaning of positive and negative values of f^2 are related to nucleophilic and electrophilic sites respectively. Like the charge distribution observed in the MEP, f^2 have opposite reactivity for each heterocyclic ring. Granting electrophilic properties to the hydrogen acceptor ring and nucleophilic properties to the opposite 1,2,3-triazole. It should be noted

that unlike the MEP, the nature of R_1 influences the disposition of the reactive centers of both heterocyclic rings.

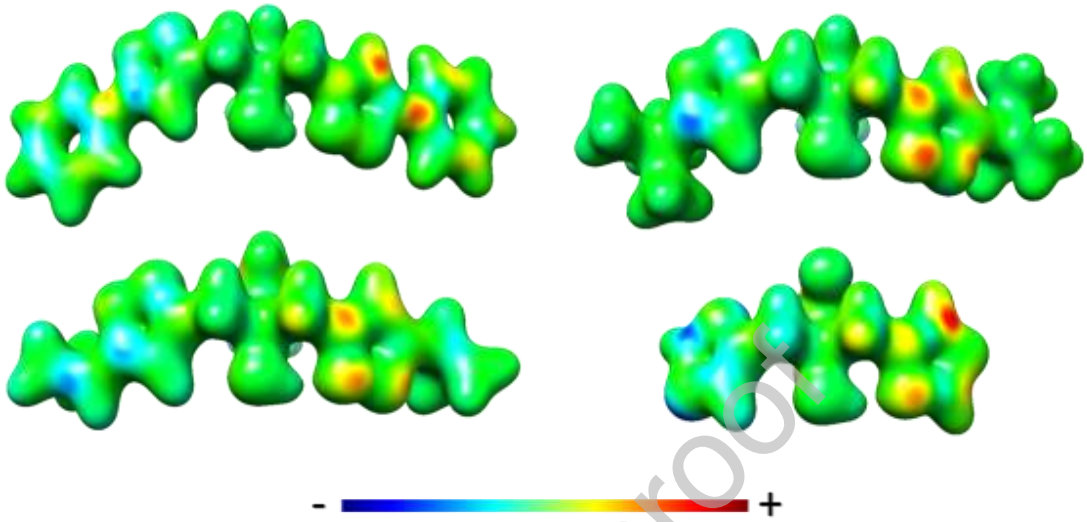

Figure 14. Representative f^2 mapped on the electron density surface with iso value of 0.05 a.u., for the set of proposed structures and for fluconazole structure calculated with the PBE0/3-21G method. The color scales from blue to red refer to values of -0.001 a.u. to 0.001 a.u. respectively.

3.3.2. Effects of S2 substituent in the molecular reactivity

The distribution of the charge density in the MEP seem invariant to S2 nature. Opposite situation is observed in the reactivity of the aromatic ring measured through f^2, being the methoxy derivatives the only species with nucleophilic features, while the rest of proposed structures this ring present electrophilic properties (figure 15).

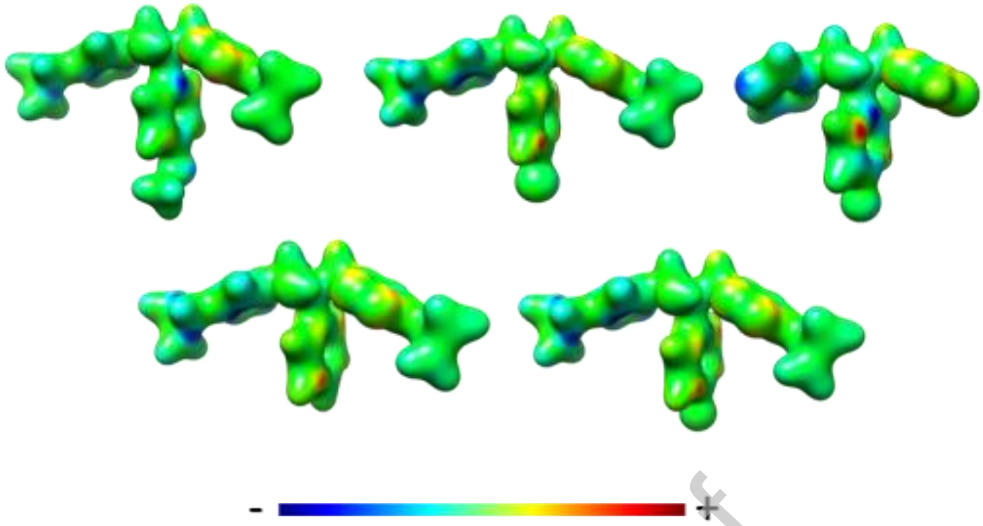

Figure 15. Representative f^2, mapped on the electron density surface with iso value of 0.05 a.u., for the set of proposed structures and for fluconazole structure calculated with the PBE0/3-21G method. The color scales from blue to red refer to values of -0.001 a.u. to 0.001 a.u. respectively.

3.3.3. Global properties

Local reactivity description usually results useful for the understanding of a chemical system. Nevertheless, some other quantities based on the global behavior can be used. An example of this are the ionization potential, **IP**, that is a measure of the electron subtraction of an electron; the electron-affinity, **EA**, that opposite to IP, is a measure of the electron acceptor capacity of a system; and the softness, ***S***, the deformation capacity of an electron density. The table 1, concentrates some energetical global parameters calculated at the DFT framework. For fluconazole structure, it is recognized that its antifungal activity is closely related to its interaction with the HEME group of the active center of cytochrome P450 protein, through coordination bonds between the Fe^{+2} atom and one of the nitrogen atoms

of the fluconazole heterocyclic ring. For this reason, it is necessary an electron donor system. Under this argument, these systems are the molecules with the highest probability to interact with the active center of cytochrome P450 protein, this due to their low IP value. However, all systems reported here show better electronic properties regarding to fluconazole structure.

Table 5. Some quantum global descriptors in eV, where Ionization Potential, PI, Electron affinity, EA, and Softness, S, of proposed bi-1,2,3-triazoles were calculated at the PBE0/3-21G method.

System	IP	EA	S	System	IP	EA	S
1.A	6.8864	0.2888	0.0758	2.D	7.3761	-0.1596	0.0664
1.B	7.0373	0.3267	0.0745	2.C	7.3819	-0.2281	0.0657
1.C	7.0793	0.3941	0.0748	3.D	7.7115	-0.1372	0.0637
1.D	7.0892	0.4265	0.0750	3.B	7.7261	-0.3236	0.0621
2.A	7.0947	-0.4004	0.0667	3.C	7.7391	-0.2096	0.0629
2.B	7.3459	-0.3480	0.0650	F	8.2659	-0.2938	0.0584
3.A	7.3640	-0.3757	0.0646				

4. Conclusions

Single crystal X ray diffraction studies of 1,3-bis-(1,2,3-triazol-1-yl)-propan-2-ol derivatives revealed an important O-H···N hydrogen bond between the hydroxyl group and one triazolyl N(3) nitrogen which is in agreement with theoretical calculations bearing a strong resemblance to Fluconazole molecule. For each compound, only one polymorph was found and to the best of our knowledge, these are the first examples about the crystal structure of this kind of compounds. Theoretical calculations indicate that a high similarity can be found between these products and the leading Flucanozole molecule; hence, a good

antifungal ability would be expected for these compounds, driving to more studies about this topic.

Competing Interests

The authors declare that they have no competing interests.

Acknowledgments

Financial support from CONACYT (Project No. A1-S-18230) is gratefully acknowledged. This work was also supported by COMECYT (fellowship for AZH). The authors would like to thank Signa S.A. de C. V. for some graciously donated solvents and reagents and to N. Zavala, A. Nuñez, L. Triana and M. C. Martínez for the technical support.

References

1.- C. Lass-Flörl, Drugs 71 (2011) 2405.

2.- A.A. Sagatova, M.V. Keniya, R.K. Wilson, B.C. Monk, J.D.A. Tyndall, Antimicrob. Agents Ch.59 (2015) 4982.

3.- N. Rodriguez-Hornedo, Mol. Pharm. 4 (2007) 299.

4.- A.V. Trask, Mol. Pharm. 4 (2007) 301.

5.- J. Kastelic, N. Lah, D. Kikelj, I. Leban, Acta Crystallogr. C C67 (2011), o370.

6.- J. Kastelic, Z. Hodnik, P. Sket, J. Plavec, N. Lah, I. Leban, M. Pajk, O. Planinsek, D. Kikelj, Cryst. Growth Des. 10 (2010) 4943.

7.- M. Karanam, S. Dev, A. R. Choudhury, Cryst. Growth Des. 12 (2012) 240.

8.- H.J. Park, M.S. Kim, S. Lee, J.S. Kim, J.S. Woo, J.S. Park, S.J. Hwang, Int. J. Pharm. 328 (2007) 152.

9.- K.A. Alkhamis, M.S. Salem, R.M. Obaidat, J. Pharm. Sci. 95 (2006) 859.

10.- M.R. Caira, K.A. Alkhamis, R.M. Obaidat, J. Pharm. Sci. 93 (2004) 601.

11.- S.R. Desai, M.M. Shaikh, S.R. Dharwadkar, Thermochim. Acta 399 (2003), 81.

12.- S. Wang, L. Zhang, Y. Jin, J. H. Tang, H. Su, S. Yu, And H. Ren, Asian J. Chem. 26 (2014) 2362.

13.- Y. Zou, Q. Zhao, J. Liao, H. Hua, S. Yu, X. Chai, M. Xu, Q. Wua, Bioorg. Med. Chem. Lett. 22 (2012) 2959.

14.- V.S. Pore, M.A. Jagtap, S.G. Agalave, A.K. Pandey, M.I. Siddiqi, V. Kumar, P.K. Shukla, MedChemComm 3 (2012) 484.

15.- N.G. Aher, V.S. Pore, N.N. Mishra, A. Kumar, P.K. Shukla, A. Sharma, M.K. Bhat, Bioorg. Med. Chem. Lett. 19 (2009) 759.

16.- V.S. Pore, N.G. Aher, M. Kumar, P.K. Shukla, Tetrahedron 62 (2006) 11178.

17.- A. Zambrano-Huerta, D. D. Cifuentes-Castañeda, J. Bautista-Renedo, H. Mendieta-Zerón, R. C. Melgar-Fernández, S. Pavón-Romero, M. Morales-Rodríguez, B. A. Frontana-Uribe, N. González-Rivas, E. Cuevas-Yañez. Med. Chem. Res. 28 (2019) 571.

18.- G. M. Sheldrick, "A short history of SHELX." Acta Crystallogr. A 64 (2008)112.

19.- C. B. Hübschle, G. M. Sheldrick and B. Dittrich. J. Appl. Crystallogr. 44 (2011) 1281.

20.- L. J. Farrugia, Ortep-3 for Windows, http://www.chem.gla.ac.uk/~louis/software/ortep/

21.- Persistence of Vision Raytracer (Version 3.6), Persistence of Vision Pty. Ltd. (2004) http://www.povray.org; (c) GIMP 2.8: The GNU Image Manipulation Program. http://www.gimp.org

22.- J. Gonzalez, V.M. Pérez, D.O. Jiménez, G. Lopez-Valdez, D. Corona, E. Cuevas-Yañez, Tetrahedron Lett. 52 (2011), 3514.

23.- A.R Katritzky, S.K. Singh, N.K. Meher, J. Doskocz, K. Suzuki, R. Jiang, G.L. Sommen, D.A. Ciaramitaro, P.J. Steel, ARKIVOC 2006, 43.

24.- M. Valiev, E. J. Bylaska, N. Govind, K. Kowalski, T. P. Straatsma, H. J. J. van Dam, D. Wang, J. Nieplocha, E. Apra, T. L. Windus, W. A. de Jong, Comput. Phys. Commun. 181 (2010) 1477.

25.- J. Lu, S. Zhu, Z, Zhu, Q. Wu and G. Zhao, Int. J. Quantum Chem. 106 (2006) 2073.

26.- L. N. Anderson, M. B. Oviedo, B. M. Wong, J. Chem. Theory Comput. 13 (2017) 1656.

27.- M. Rocha, A. A. Di Santo, J. M. Arias, D. M. Gil, A. B. Altabef, Spectrochim. Acta A 136B (2015) 635.

28.- J. I. Martínez-Araya, J. Math. Chem. 53 (2014) 2.

29.- J. K. R da Silva, J. R. Silva, S. B. Nascimento and S. F. M da Luz, Molecules, 19 (2014) 17942.

30.- L. R. Peyton, S. Gallagher and M. Hashemzadeh, Drugs Today 51 (2015) 705.

31.- C. M. Orben, B. Dittrich, Acta Crystallogr. C C70 (2014) 580.

32.- I. A. Novakov, A. S. Babushkin, A. S. Yablokov, M. B. Nawrozkij, O. V. Vostrikova, D. S. Shejkin, A. S. Mkrtchyan, K. V. Balakin, Russ. Chem. B. 67 (2018) 395.

33.- T. T. Talele, J. Med. Chem. 59 (2016) 8712.

34.- S. J. Chawner, M. J. Cases-Thomas, J. A. Bull, Eur. J. Org. Chem. (2017) 5015.

35.- J. Salaün, Top. Curr. Chem. 207 (2000) 1.

36.- C. J. Suckling, Angew. Chem. Int. Ed. 27 (1988) 537.

37.- B. Schulze, U.S. Schubert, Chem. Soc. Rev. 43 (2014) 2522.

38.- S. Fernicola, I. Torquati, A. Paiardini, G. Giardina, G. Rampioni, M. Messina, L. Leoni, F. Del Bello, R. Petrelli, S. Rinaldo, L. Cappellacci, F. Cutruzzolà J. Med. Chem. 58 (2015) 8269.

39.- V. Haridas, S. Sahu, P. Kumar P.P., A. R. Sapala, RSC Adv. 2 (2012) 12594.

40.- M. T. Ramírez-Palma, J. Segura-Arzate, G. López-Téllez, E. Cuevas-Yañez, J. Chem. (2016) 6432492. http://dx.doi.org/10.1155/2016/6432492